Pergamon

Cement and Concrete Research 29 (1999) 1887–1892

CEMENT AND CONCRETE RESEARCH

Fracture process zone of notched three-point-bending concrete beams

D. Zhang[1], K. Wu*

Tongji University, School of Materials, Science & Engineering, State Key Laboratory of Concrete Materials Research, Siping Road 1239, Shanghai 200092, People's Republic of China

Received 13 January 1999; accepted 17 August 1999

Abstract

By measuring and analyzing the load-deflection curve and acoustic emission characteristics of notched three-point-bending concrete beams with different notch depths, the length of the fracture process zone (FPZ) was calculated from the difference between the equivalent crack lengths obtained by different kinds of equivalence. Then, the evolution of the FPZ was quantitatively described. It was found that length of the FPZ is not a material parameter; it is greatly influenced by the specimen size. But in a relative sense, the influence of the specimen size can be eliminated. Also, the evolution of the FPZ in specimens of different sizes is almost the same. When the crack length is small, the FPZ increases linearly with the crack extension. As the crack extends to half of the ligament, the FPZ reaches its maximum size. Thereafter, the FPZ moves ahead and shrinks, but the ratio of its length to the length of the residual ligament remains constant, approximately equal to 0.77.

Keywords: Crack detection; Fracture process zone; Mechanical properties; Concrete

1. Introduction

The fracture process zone (FPZ) is one of the hottest topics in the field of concrete fracture mechanics. One reason why linear elastic fracture mechanics (LEFM) is invalid for concrete is the presence of the FPZ [1,2]. Furthermore, fracture parameters such as fracture toughness (K_{IC}) and fracture energy (G_f) are size-dependent and even contradict test data from different experiments, which seriously hinders the application of fracture mechanics to concrete in structural analysis, design, and safety assessment. The existence of the FPZ in front of an extending crack in concrete may be the intrinsic reason for the size dependence of the fracture parameters. So it is significant to measure the size of the FPZ and its evolution during crack extension and to investigate the role of the FPZ in the size dependence of fracture parameters. Finally, the goal is to obtain size-independent fracture parameters for the application of fracture mechanics of concrete.

Because of the complexity of the internal structure of concrete, there remains some debate about the FPZ in concrete, with questions such as: "Is the size of FPZ a material parameter?" and "Does it depend on the shape and size of the specimens?" There are only some qualitative results concerning the evolution of the FPZ. Nevertheless, the quantitative description of evolution of the FPZ is a prerequisite for determination of size-independent fracture parameters. In this paper, by measuring the load-deflection curves and acoustic emission (AE) characteristics of notched three-point-bending (TPB) concrete beams, the length of the FPZ is calculated and the evolution of the FPZ during crack extension is quantitatively described.

2. Measurement of load-deflection curves and AE characteristics of notched TPB concrete beams

High-strength concrete with the following materials was used: 525 normal silicate cement, ultrafine slag powder with a specific surface area of 600m^2/kg, fly ash, sand, and crushed stone. The mix proportions were water:cement:fly ash:ultrafine slag powder:sand:crushed stone = 0.27:0.6:0.17:0.27:1.24:1.87. A high-range water reducer (a sodium salt of a condensed naphthalenesulphonic acid) was used in the amount of 1% by weight of cement.

The size of the notched concrete beam was 515 × 100 × 100 mm^3. The ratio of span to depth was 4. The notch depth varied from 20 to 80 mm. Cubic specimens were used to measure the compressive strength and splitting tensile strength. The measurement of load-deflection curves was

* Corresponding author. Tel.: +86-21-6598-2412; fax: +86-21-6598-3465.

E-mail address: zhangdng@ust.hk (D. Zhang)

[1]D. Zhang is currently with the Department of Civil Engineering, Hong Kong University of Science and Technology, Clear Water Bay, Kowloon, Hong Kong.

0008-8846/99/$ – see front matter
PII: S0008-8846(99)00186-6

achieved by means of an Instron 8501 testing machine (Instran, Canton, MA, USA). Midspan deflection of the concrete beam was chosen as the controlling parameter in the measurements. The loading rate was 0.025 mm/min. AE characteristics were measured by means of a PAC Spartan 2000 (Physical Acoustics, Princeton, NJ, USA). The two systems were connected by cables so that the load-deflection curves and AE characteristics could be recorded simultaneously. Fig. 1 shows the testing systems. The mechanical properties of the concrete are given in Table 1.

The load-deflection curves of notched TPB concrete beam with different notch depths are shown in Fig. 2. Fig. 3 shows its AE characteristics. It is obvious in these figures that as the notch depth decreases, the descending branch of the load-deflection curve becomes steeper. The shape and position of the peak in the AE records also change with notch depth. In fact, as the notch depth increases, the peak of the AE records becomes lower and wider, and moves along the horizontal axis. When the notch depth is 80 mm, no visible peak is found in AE records. This indicates that as the notch depth increases, the fracture process in concrete beam becomes less catastrophic.

3. Equivalent crack extension

3.1. Stiffness and compliance of notched TPB concrete beam

The midspan deflection (δ) of a TPB beam can be written as Eq. (1):

$$\delta = \frac{P \cdot s^3}{4w \cdot h^3 \cdot E} \tag{1}$$

where P = external load at midspan, s = span, w = thickness, h = height of the specimen, and E = elastic modulus.

For a notched TPB beam, the midspan deflection can be written as the sum of two parts [3], as seen in Eq. (2).

$$\delta = \delta_{cr} + \delta_{nc} \tag{2}$$

where δ_{nc} is the deflection caused by bending of the beam [see Eq. (3)]:

Table 1
Mechanical properties of concrete

Compressive strength (MPa)	Tensile strength (MPa)	Fracture energy (N/m)	Elastic modulus (GPa)	Characteristic length[a] (m)
96.7	6.12	196.3	45.2	0.24

[a] Characteristic length: $l_{ch} = E \cdot G_f / f_t^2$, where E is the elastic modulus, G_f is the fracture energy, and f_t is the tensile strength.

$$\delta_{nc} = \frac{P \cdot s^3}{4w \cdot h^3 \cdot E} \tag{3}$$

and δ_{cr} is the deflection caused by the notch [see Eq. (4)]:

$$\delta_{cr} = \frac{3P \cdot s^2 \cdot V(a_o/h)}{2w \cdot h^2 \cdot E} \tag{4}$$

where [see Eq. (5)]

$$V(a_o/h) = \left(\frac{a_o/h}{1 - a_o/h}\right)^2 \cdot \left[5.58 - 19.57(a_o/h) + 36.82(a_o/h)^2 - 34.94(a_o/h)^3 + 12.77(a_o/h)^4\right] \tag{5}$$

and a_o = notch depth.

Thus, the initial compliance and stiffness of a notched TPB beam can be written as Eq. (6) and Eq. (7):

$$C = \delta/P = \frac{s^3}{4w \cdot h^3 \cdot E} + \frac{3s^2}{2w \cdot h^2 \cdot E} \cdot V(a_o/h) \tag{6}$$

$$S = 1/C \tag{7}$$

Fig. 4 shows the comparison between test data and Eq. (7). It can be seen that Eqs. (6) and (7) are accurate.

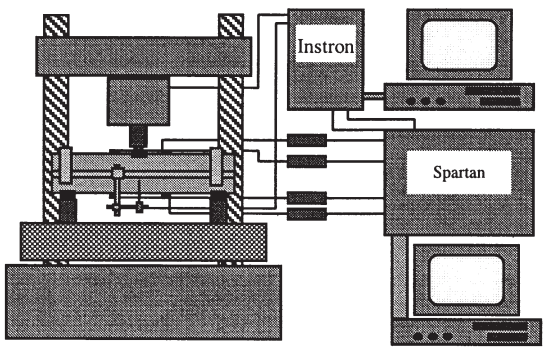

Fig. 1. Testing systems.

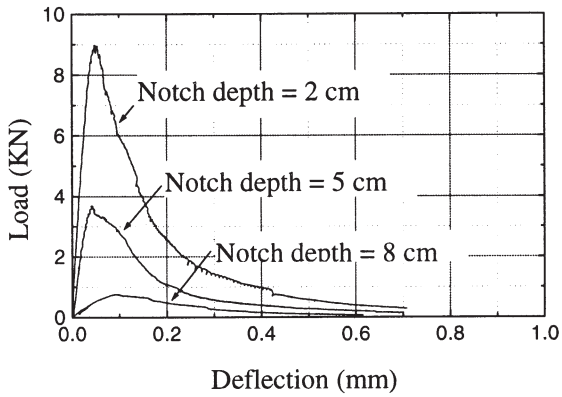

Fig. 2. Load-deflection curves.

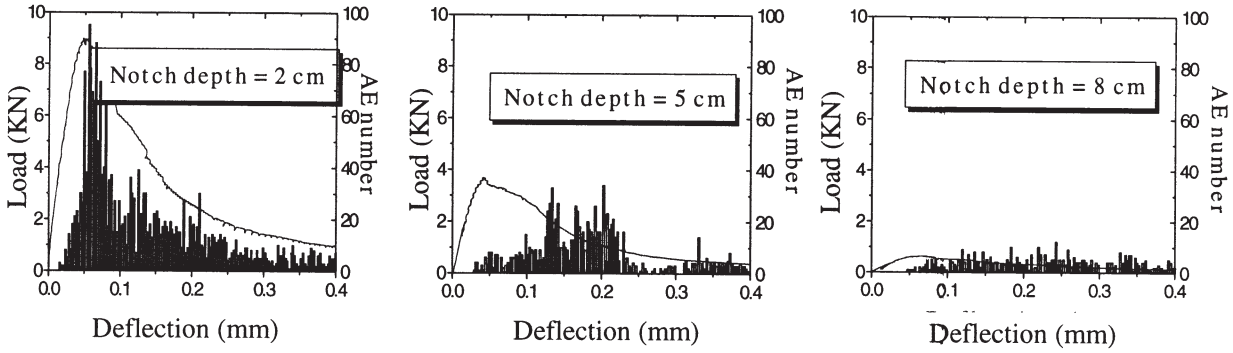

Fig. 3. AE records and load-deflection curve.

3.2. Calculation of equivalent crack

The damage process of concrete due to external forces involves the emergence, development, and movement of the FPZ. Meanwhile, as material in the FPZ deteriorates, its elastic modulus decreases, which causes the compliance of the specimen to increase.

According to stiffness equivalence, the equivalent crack length ($a_{P-\Delta}$) at different loading stage can be calculated using Eq. (7). The calculated results are shown in Fig. 5. Fig. 5 also shows the calculated results of crack length (a_{AE}) according to the equivalence of AE event records [see Eq. (8)].

$$a_{AE} = a_o + \Delta a = a_o + \frac{N_\delta}{N_{total}} \tag{8}$$

where N_δ = the cumulative number of AE events at deflection δ, and N_{total} = the total number of AE events. It is found that the crack lengths calculated by these two methods are different.

4. Evolution of FPZ

The reason why the calculated results of crack length differ by the two different methods may be that a sharp, well-defined crack tip in concrete does not exist at all. In fact, in front of the crack in concrete there is a damage zone without a clear boundary, which is normally called the fracture process zone. The results of crack extension calculated by different methods are only some sort of equivalence to the damage occurring in the FPZ. For example, $a_{P-\Delta}$ is obtained from the stiffness equivalence, and a_{AE} from the AE event records equivalence.

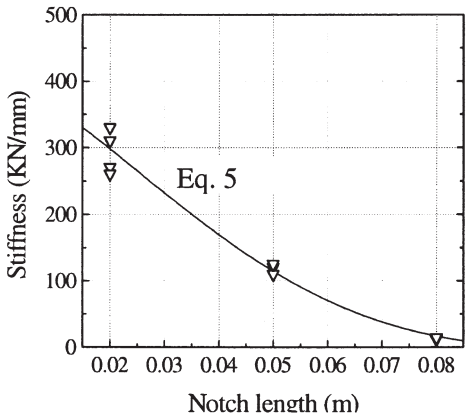

Fig. 4. Eq. (7) and testing data of stiffness.

As shown in Fig. 6, the equivalent crack ($a_{P-\Delta}$) determined from stiffness equivalence is composed of three segments, as seen in Eq. (9)

$$a_{P-\Delta} = a_o + \Delta a' + \Delta a'' \tag{9}$$

where a_o = notch depth, $\Delta a'$ = traction-free crack segment, the crack segment equivalent to FPZ according to stiffness equivalence $\Delta a'''$ is assumed to be proportional to the length of FPZ [see EQ. (10)]:

$$\Delta a'' = \gamma \cdot l_{FPZ} \tag{10}$$

Similarly, the crack length obtained according to AE records can also be formulated as sum of three parts, as shown in Eq. (11):

$$a_{AE} = a_o + \Delta a' + \Delta a''' \tag{11}$$

where $\Delta a'''$ = crack segment equivalent to FPZ according to AE records, and is assumed to be proportional to the length of the FPZ [see Eq. (12)].

$$\Delta a''' = \eta \cdot l_{FPZ} \tag{12}$$

Thus, the difference between the crack lengths calculated by the two kinds of equivalence is shown in Eq. (13).

$$\delta a = a_{P-\Delta} - a_{AE} = (\gamma - \eta) \cdot l_{FPZ} \tag{13}$$

The FPZ reaches a maximum when it reaches its peak. So according to δa, we can discover something about the evolution of the FPZ. First, in Fig. 7, taking $\delta a = a_{P-\Delta} - a_{AE}$ as the ordinate, $\Delta a_{P-\Delta}$/ligament as the abscissa, we find that the equivalent crack extension at the saturation of the FPZ is 3.84 cm for a notch depth of 2 cm, 2.55 for a notch depth of 5 cm, and 1.02 for a notch depth of 8 cm, respectively.

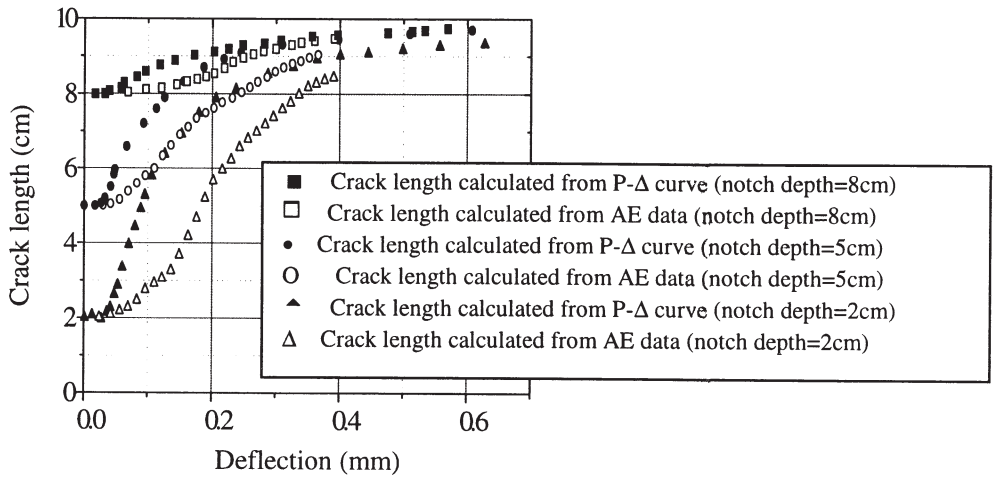

Fig. 5. Calculated equivalent crack results.

Assume that the stress-strain curve of concrete takes a bi-linear form. The ascending branch is shown in Eq. (14).

$$0 \leqslant \varepsilon < \varepsilon_o: \quad \sigma = E_o \cdot \varepsilon \tag{14}$$

The descending branch is [see Eq. (15)]:

$$\varepsilon_o \leqslant \varepsilon < \varepsilon_\infty: \quad \sigma = f_t \cdot \frac{\varepsilon_\infty - \varepsilon}{\varepsilon_\infty - \varepsilon_o} \tag{15}$$

The elastic modulus of the ascending branch is E_o. The secant modulus of descending branch is [see Eq. (16)]:

$$E = \frac{1}{\alpha} \cdot \frac{\varepsilon_\infty - \varepsilon}{\varepsilon} \cdot E_o \qquad \alpha = \frac{\varepsilon_\infty - \varepsilon_o}{\varepsilon_o} \tag{16}$$

The distributions of strain and elastic modulus as shown in Fig. 8a are [see Eq. (17)]:

$$\varepsilon(x) = (1 + \alpha \cdot \frac{x}{l_{\mathrm{FPZ}}}) \cdot \varepsilon_o \tag{17}$$

and [see Eq. (18)]:

$$E(x) = \frac{1 - x/l_{\mathrm{FPZ}}}{1 + \alpha \cdot (x/l_{\mathrm{FPZ}})} \cdot E_o \tag{18}$$

To calculate the stiffness of FPZ, we take a cross-section with variable width as shown in Fig. 8b as equivalent to the FPZ [see Eq. (19)]:

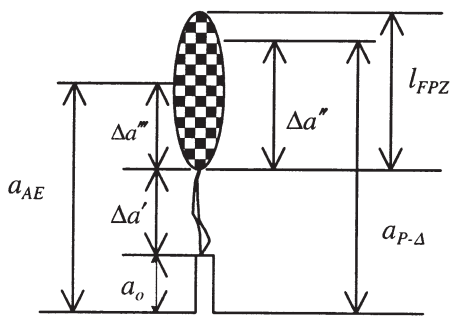

Fig. 6. Equivalence of FPZ.

$$E = \frac{w(x)}{w_o} \cdot E_o = \frac{1 - x/l_{\mathrm{FPZ}}}{1 + \alpha \cdot (x/l_{\mathrm{FPZ}})} \cdot E_o \tag{19}$$

So the variable width of the cross section is [see Eq. (20)]:

$$w(x) = \frac{1 - x/l_{\mathrm{FPZ}}}{1 + \alpha \cdot (x/l_{\mathrm{FPZ}})} \cdot w_o \tag{20}$$

and its height is [see Eq. (21)]:

$$x = \frac{1 - w/w_o}{1 + \alpha \cdot (w/w_o)} \cdot l_{\mathrm{FPZ}} \tag{21}$$

and its stiffness S_1 is [see Eq. (22)]:

$$S_1 = \int_0^{w_o} \frac{4E_o \cdot x^3}{s^3} \cdot dw \tag{22}$$

Combining Eqs. (21) and (22) and integrating the right side of Eq. (22), we obtain Eq. (23):

$$S_1 = f(\alpha) \cdot \frac{4E_o \cdot w_o \cdot l_{\mathrm{FPZ}}^3}{s^3}$$

$$f(\alpha) = \frac{1}{2\alpha^4} \cdot [(\alpha + 1)^3 - 6(\alpha + 1)^2 + 5(\alpha + 1) + 6(\alpha + 1) \cdot \ln(\alpha + 1) - 2\alpha)] \tag{23}$$

According to stiffness equivalence, the stiffness of the equivalent crack S_2 is equal to S_1 [see Eq. (24)]:

$$S_2 = \frac{4E_o \cdot w_o \cdot (l_{\mathrm{FPZ}} - \Delta a_{P-\Delta})^3}{s^3} = S_1 = f(\alpha) \cdot \frac{4E_o \cdot w_o \cdot l_{\mathrm{FPZ}}}{s^3} \tag{24}$$

So, we obtain Eq. (25):

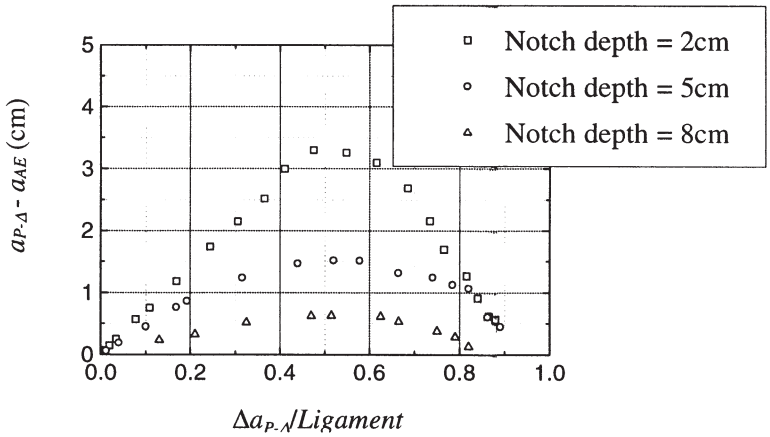

Fig. 7. $a_{P-\Delta} - a_{AE}$ vs. $\Delta a_{P-\Delta}$/ligament.

$$\Delta a_{P-\Delta} = [1 - \sqrt[3]{f(\alpha)}] \cdot l_{FPZ} \tag{25}$$

and Eq. (26):

$$l_{FPZ} = \frac{\Delta \alpha_{P-\Delta}}{1 - \sqrt[3]{f(\alpha)}} \tag{26}$$

Assuming that the width of the FPZ is three times the maximum size of the aggregate, the parameters of the bilinear stress-strain curve can be determined according to the mechanical properties listed in Table 1 [see Eq. (27)]:

$$f_t = 6.12 \text{ MPa}, E_o = 45.2 \text{ GPa}, \varepsilon_o = \frac{f_t}{E_o} = 135.4 \times 10^{-6}, w_{FPZ} = 0.045 \text{ m}, \Delta\varepsilon = \varepsilon_\infty - \varepsilon_o = \frac{2g_f}{f_t} = \frac{2(G_F/w_{FPZ})}{f_t} = 1426 \times 10^{-6}, \alpha = \frac{\Delta\varepsilon}{\varepsilon_o} \approx 10 \tag{27}$$

So [see Eq. (28)]:

$$\Delta a_{P-\Delta} = 0.7 l_{FPZ}$$
$$l_{FPZ} = 1.43 \Delta a_{P-\Delta} \tag{28}$$

The length of the saturated FPZ and the factor ($\gamma - \eta$) can be determined according to the above equations and the equivalent crack extension at the saturation of the FPZ. It is obvious in Table 2 that the size of the FPZ depends greatly on the size of the ligament.

Using the factor ($\gamma - \eta$), we can calculate the evolution of the FPZ for different specimen sizes (ligament size). In Fig. 9, the relative crack extension ($\Delta a_P - \Delta$/initial length of ligament) is taken as the abscissa, the relative length of FPZ (l_{FPZ}/initial length of ligament) as the ordinate. Although specimen size influences the size of the FPZ greatly, the evolutions in relative form of the FPZ for three specimen sizes are almost the same. In the range of this work, when the equivalent crack is small, the relative length of the FPZ increases linearly with relative crack extension. When the crack extends about half of the ligament, the FPZ becomes saturated and maximum in size, and occupies probably 70% of the initial length of ligament. Thereafter, the saturated FPZ moves ahead and shrinks as the crack extends further.

Although the length of the FPZ decreases after saturation, the length of the remaining ligament also decreases, and they decrease at nearly the same rate. If we take the ra-

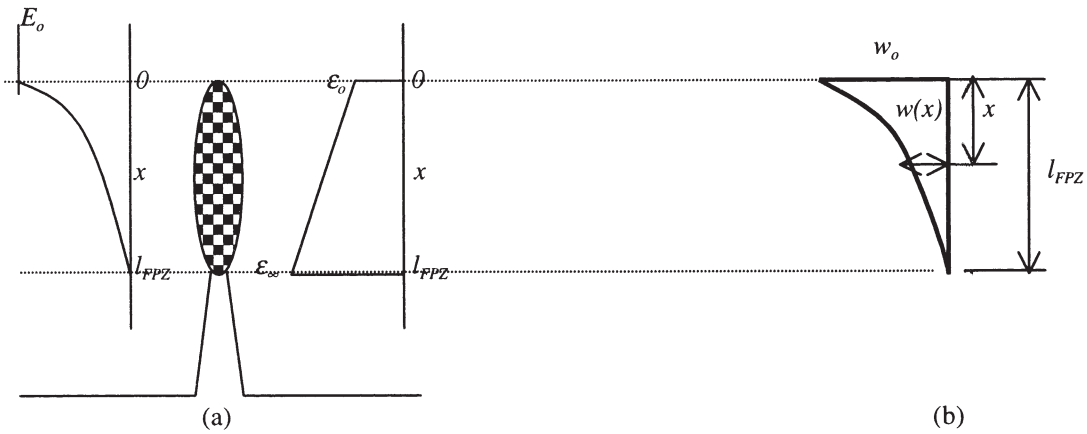

Fig. 8. Analysis of FPZ.

Table 2
The length of FPZ and factor ($\gamma - \eta$) of notched TPB concrete beam with different notch depths

Notch depth (cm)	Ligament length (cm)	Length of saturated FPZ (cm)	($\gamma - \eta$)
2	8	5.49	0.60
5	5	3.65	0.42
8	2	1.46	0.43

tio of FPZ length to the length of residual ligament as the ordinate (in Fig. 10), it may be found that after saturation the ratio remains constant, approximately 0.77.

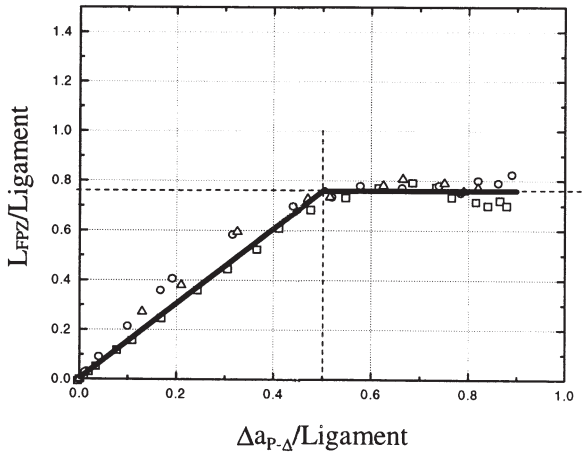

Fig. 10. Change of length of FPZ in concrete.

5. Conclusions

From analyses of the load-deflection curves and AE characteristics of notched TPB concrete beams, stiffness and AE record equivalence are used to calculate the crack extension. The calculated results using different kinds of equivalence are different. From this difference, the size and evolution of the FPZ can be determined.

The length of the FPZ, which depends greatly on specimen size, is not a material parameter. But in relative form, the influence of specimen size can be eliminated, and the evolution of the FPZ for different specimen size is almost the same.

When the crack extension is small, the length of the FPZ increases linearly with crack extension. When the crack extends half of the ligament, the FPZ becomes maximum and saturated and occupies about 70% of the initial length of the ligament. Thereafter, the FPZ moves ahead and shrinks, but the ratio of the saturated FPZ length to the length of the residual ligament remains constant, approximately 0.77.

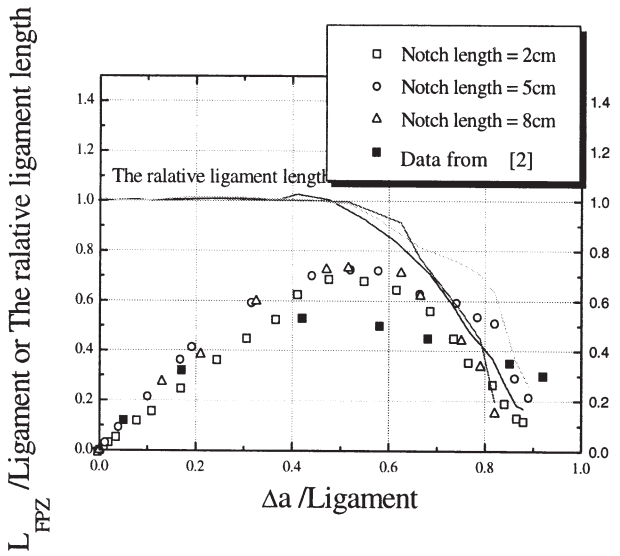

Fig. 9. Change of length of FPZ in concrete.

References

[1] S. Mindess, Fracture process zone detection, in: S. P. Shah (Ed.), Fracture Mechanics Test Methods for Concrete (Report of RILEM FMT-89), Chapman & Hall, London, 1991, pp. 231–261.
[2] F.H. Wittmann, X. Hu, Fracture process zone in cementitious materials, Int J Fract 51 (1991) 3–18.
[3] H. Tada, P.C. Paris, G.R. Irwin, Stress Analysis of Cracks Handbook, Del Research Corporation, Hellertown, USA, 1973.